Supporting Information

Visualization of peroxynitrite/GSH cross-talk in the oxidant-antioxidant balance by a dual-fluorophore and dual-site based mito-specific fluorescent probe

*Yu Liu[1], Jinjin Zhao[1], Yingzhe Wang**

Table of Contents

Materials and methods. All the reagents used in this work were got from suppliers without additional purification. ^{13}C NMR and ^{1}H NMR spectra were all recorded on the JNM-ECS-400 MHz. Mass spectrums (ESI) were performed on Bruker Micro TOF ESI-TOF Mass Spectrometer. The high-resolution mass spectrometry (HRMS) was carried out by a Bruker microTOF-Q II mass spectrometer. Fluorescence spectrums were measured by a Hitachi F-7000 spectrofluorophotometer with both excitation and emission slit widths set at 5.0 nm. The UV-vis spectrums were performed on the Agilent Technologies Cary 5000 Series UV-vis-NIR spectrophotometer. The two-photon absorption was measured using the integrating sphere on FLS920 of Edinburgh Instruments. Cell imaging was got from the Olympus confocal fluorescence microscopy (FV1000 MPE).

UV-vis and fluorescence spectral measurements. The stock solution of **CD-NA** (10^{-3} mol/l) was prepared in DMSO. ROS and RSS were all prepared by the reported papers in water. In the process of testing, the solution of **CD-NA** (10 μM, 2 mL) diluted in PBS (0.01 M, 20% EtOH, pH 7.4) was filled into a quartz optical cell. The other specimens to be tested were added respectively by the micropipettes. The excitation of measurements was provided at 420 nm or 600 nm, and the excitation/emission slit widths were all set as 5.0 nm.

The procedures for the preparing ROS and RSS are listed below[1].

Peroxynitrite ($ONOO^-$): To a mixture of H_2O_2 (30 %, 0.3 ml) and concentrated H_2SO_4 (98 %, 0.08 ml) in redistilled H_2O (5 ml), the solution of $NaNO_2$ (0.2 g) in ultrapure water (5 ml) was added rapidly. Then the obtained mixture was poured into NaOH aqueous solution (0.5 g, 10 mL) immediately and MnO_2 (0.08 g) was introduced to remove excess H_2O_2. The resulting solution was filtered to afford $ONOO^-$.

Hydrogen peroxide (H_2O_2): The H_2O_2 was purchased from commercial suppliers and diluted by water.

Hypochlorite (ClO^-): The ClO^- was obtained from sodium hypochlorite which was purchased from commercial suppliers and diluted by water.

Superoxide ($O_2^{\bullet-}$): $O_2^{\bullet-}$ was generated from KO_2 which was dissolved in DMSO.

Hydroxyl radical (•OH): •OH was prepared by the mixture of H_2O_2 and 10 eq. $(NH_4)_2Fe(SO_4)_2$.

Nitric Oxide (NO): NO was generated from the aqueous solution of Na_2 [Fe $(CN)_5$ NO]•$2H_2O$.

Nitrite (NO_2^-): NO_2^- was prepared from the aqueous solution of sodium nitrite ($NaNO_2$).

Sulfuretted Hydrogen (H_2S): The H_2S was prepared by sodium sulphide (Na_2S) in deionized water.

Bisulfite ion (HSO_3^-): The HSO_3^- was prepared by sodium hydrogen sulfite ($NaHSO_3$) in deionized water.

Thiosulfate ($S_2O_3^{2-}$): The $S_2O_3^{2-}$ prepared by sodium thiosulfate ($Na_2S_2O_3$) in deionized water.

Sulfate Radical (SO_4^{2-}): The SO_4^{2-} was prepared by sodium sulfate (Na_2SO_4) in deionized water.

Glutathione (GSH), Cysteine (Cys), Homocysteine (Hcy), Histidine (His), Isoleucine(Iso), Leucine (Leu), Lysine (Lys), Methionine (Met), and Serine (Ser): These amino acid were all prepared in deionized water.

The spectrophotometric method for determining the precise concentration of $ONOO^-$ has also been listed[2].

Peroxynitrite ($ONOO^-$): The absorbance of the solution was measured at 302 nm, and the concentration of $ONOO^-$ was further obtained by the formula $[ONOO^-]=Abs_{302\ nm}/1.67$ (mM).

Cytotoxicity study. The MTT assay was conducted to evaluate the cytotoxicity. The solutions of **CD-NA** at different concentrations (0, 2, 5, 10, 20 and 50 μM) were all evaluated in HepG2 cells for 24 h according to the published literature.

Cell fluorescence imaging. HepG2 cells were selected to assess the applicability of **CD-NA**. The cells were incubated in the atmosphere of 5% CO_2 for 8 h and then treated with **CD-NA** (10 μM) for 30 min. For the investigation of **CD-NA** for GSH, the cells were incubated with **CD-NA** (10 μM) for 30 min and then treated with GSH (3 mM) for 10 min. To investigate the generating of endogenous $ONOO^-$, the cells were firstly incubated with bacterial endotoxin lipopolysaccharide (LPS) (1 μg/mL) for 14 h, followed by the addition of the **CD-NA** (10 μM) for another 30 min. As

the control experiment, the HepG2 cells were also pretreated with 2,2,6,6-tetramethylpiperidine-N-oxyl (TEMPO) (300 μM) for 30 min and then incubated with LPS (1 μg/mL) for 14 h and **CD-NA** (10 μM) for 30 min. To explore the imaging performance of **CD-NA** at the organelle level, the cells were incubated with **CD-NA** (10 μM) for 30 min and treated with Mito-tracker Green or Lyso-tracker Green (2 μM) for another 10 min. All the cells were washed with PBS buffer (pH 7.4, 0.1 M) for three times to remove the free dye before imaging. The HepG2 cells loaded with **CD-NA** were excited at 850, 559 or 405 nm. The cells stained by Mito-tracker Green and Lyso-tracker Green were excited at 488 nm. The emission was collected in the red channel (620-670 nm) and green channel (445-495 nm) using the Olympus FV1000 laser confocal scanning microscope.

In the end, we examined the ability of **CD-NA** to visualize the production of $ONOO^-$ in a drug-induced hepatotoxicity model in HepG2 cells. The cells were incubated with **CD-NA** (10 μM) for 30 min and then incubated with antipyretic acetaminophen (APAP) (100 μM) for 30 min. Furthermore, as the control experiment, the HepG2 cells were pretreated with N-acetyl cysteine (NAC) (100 μM) for 30 min before incubated with APAP (500 μM).

Response mechanism. Based on the reported literature, the speculative response mechanism of CD-NA to $ONOO^-$ and GSH was proposed and displayed (Fig. S1, S4). When adding $ONOO^-$, the oxonium group of **CD-NA** suffered from nucleophilic reaction, denitration and oxidative cleavage, and finally got a carboxylic acid product. The mass spectrum of **CD-NA** in the presence of $ONOO^-$ was shown in figure S2. The mass spectrum of the carboxylic acid product (MS: 600.16) and the simulated data (MS: 600.16) were shown in figure S3. When adding GSH, the sulfoxide group of CD-NA suffered from nucleophilic got a reduce product. The mass spectrum of CD-NA in the presence of GSH was shown in figure S5. The mass spectrum of the reduce product (MS: 873.31) and the simulated data (MS: 873.31) were shown in figure S6.

Synthetic procedures of CD-NA.

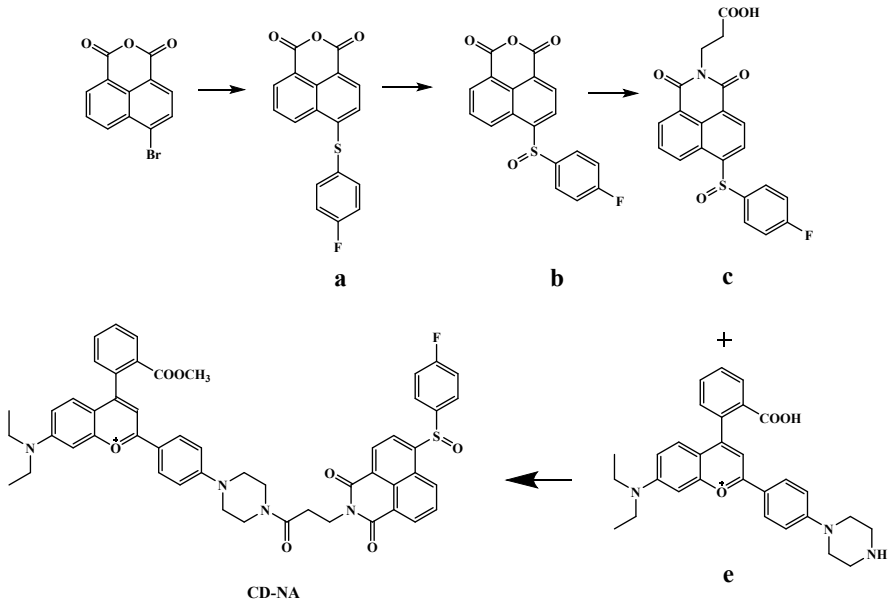

Figure S1. The synthetic procedures of **CD-NA**.

Synthesis of CD-NA. These compounds a, b, c and e have been provided in the literatures [3-6]. The compound **e** was synthesised by the published literatures. **c** (1 mmol) was added into the CH_2Cl_2 solution (20 ml) of **e** (2 mmol), HATU (2 mmol) and trimethylamine (40 μl), and then stirred for 4 h under argon protection. Then, the reaction mixture was evaporated under reduced pressure and purified by silica gel to give the pure product **CD-NA** as a mulberry solid (0.29 g, 33 %). ^{1}H NMR (400 MHz,) δ 8.70 (d, J = 7.6 Hz, 1H), 8.58 (d, J = 7.2 Hz, 1H), 8.45 (t, J = 8.2 Hz, 1H), 8.18 (d, J = 7.8 Hz, 1H), 8.09 (d, J = 9.1 Hz, 1H), 7.83 – 7.74 (m, 1H), 7.72 – 7.63 (m, 1H), 7.40 (d, J = 7.5 Hz, 1H), 7.30 (s, 1H), 7.16 (d, J = 9.4 Hz, 1H), 7.13 – 7.06 (m, 1H), 6.99 (d, J = 9.1 Hz, 1H), 6.94 (dd, J = 9.5, 2.1 Hz, 1H), 4.51 – 4.44 (m, 1H), 3.74 (d, J = 5.5 Hz, 1H), 3.62 (dd, J = 14.0, 6.9 Hz, 1H), 3.55 (d, J = 4.0 Hz, 1H), 2.85 – 2.78 (m, 1H), 1.32 (t, J = 7.0 Hz, 1H). ^{13}C NMR (101 MHz, CDCl3) δ 169.47, 166.67, 166.00, 165.88, 163.48, 163.35, 163.28, 161.58, 158.29, 154.94, 154.78, 147.79, 139.66, 136.14, 133.25, 131.95, 131.28, 131.21, 130.81, 130.54, 129.85, 129.40, 129.19, 128.55, 128.47, 128.43, 128.22, 128.13, 127.50, 125.08, 123.69, 123.36, 117.35, 117.15, 117.13, 116.02, 115.19, 114.08, 108.71, 96.87, 77.16, 52.78, 46.34, 46.19, 46.05, 44.80, 40.80, 36.91, 31.60, 12.67. HRMS (M^+) found, 889.3043; calculated for $C_{52}H_{46}FN_4O_7S^+$, 889.3066.

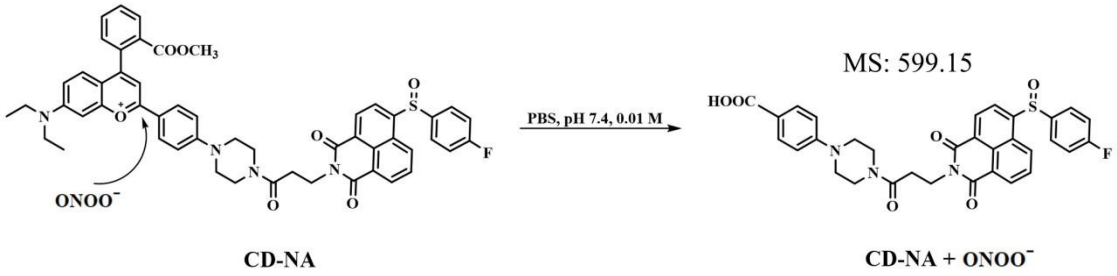

Figure S2. The proposed reaction mechanism of **CD-NA** and $ONOO^-$.

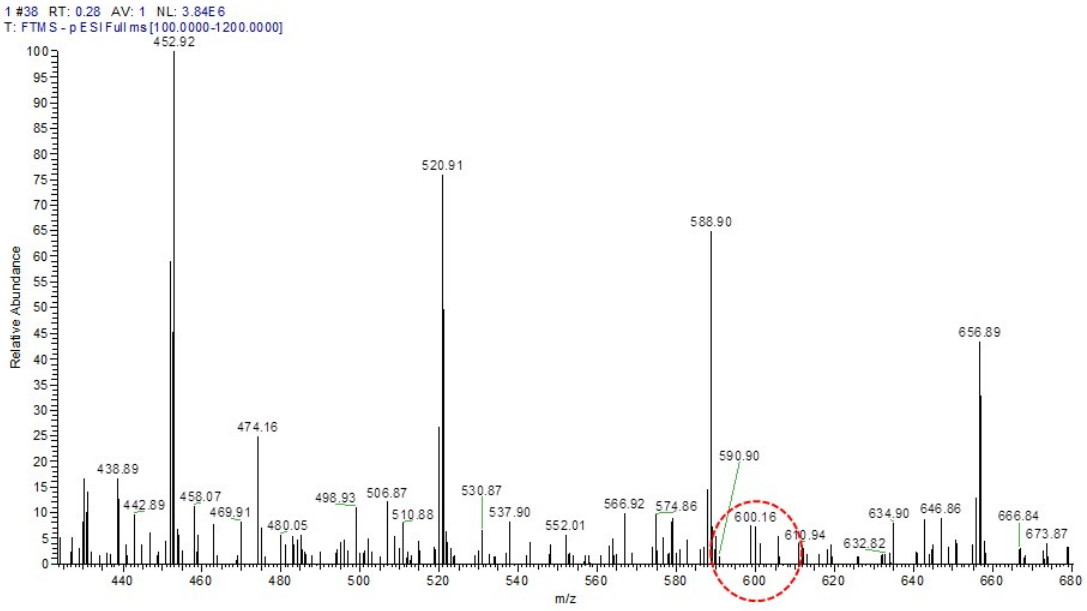

Figure S3. The mass spectrum of **CD-NA** in the presence of $ONOO^-$.

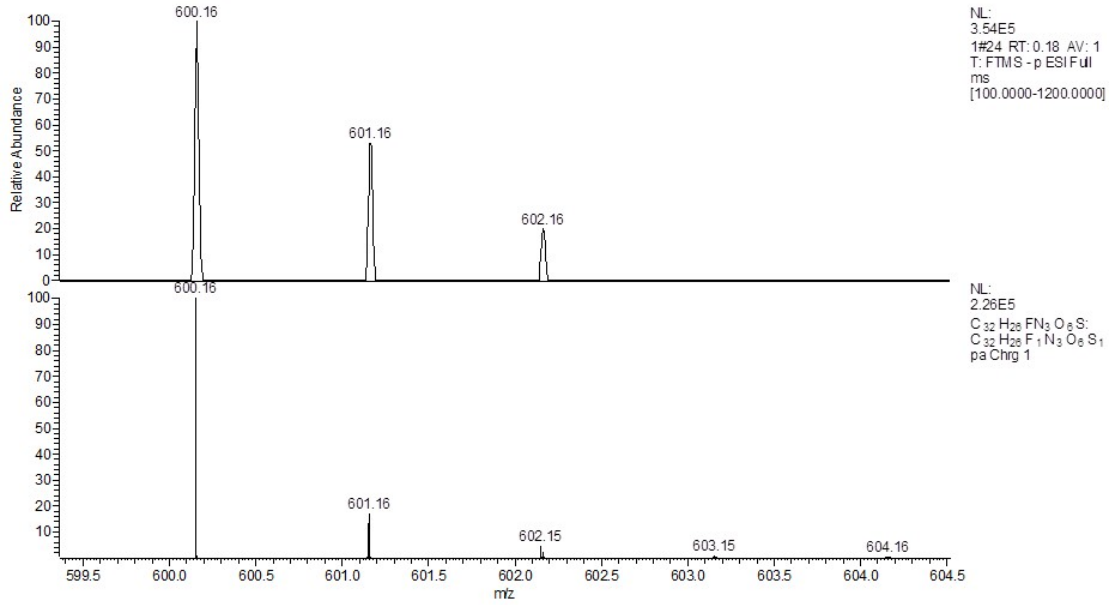

Figure S4. The mass spectrum of **CD-NA** in the presence of $ONOO^-$ and its simulated data.

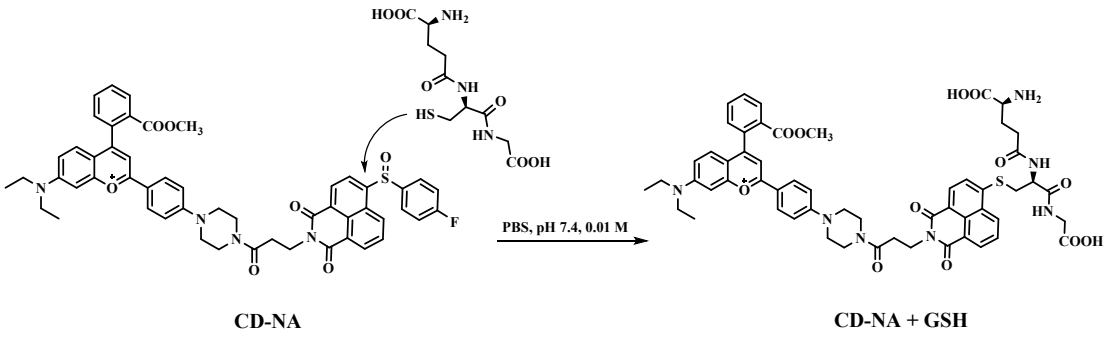

Figure S5. The proposed reaction mechanism of **CD-NA** with GSH.

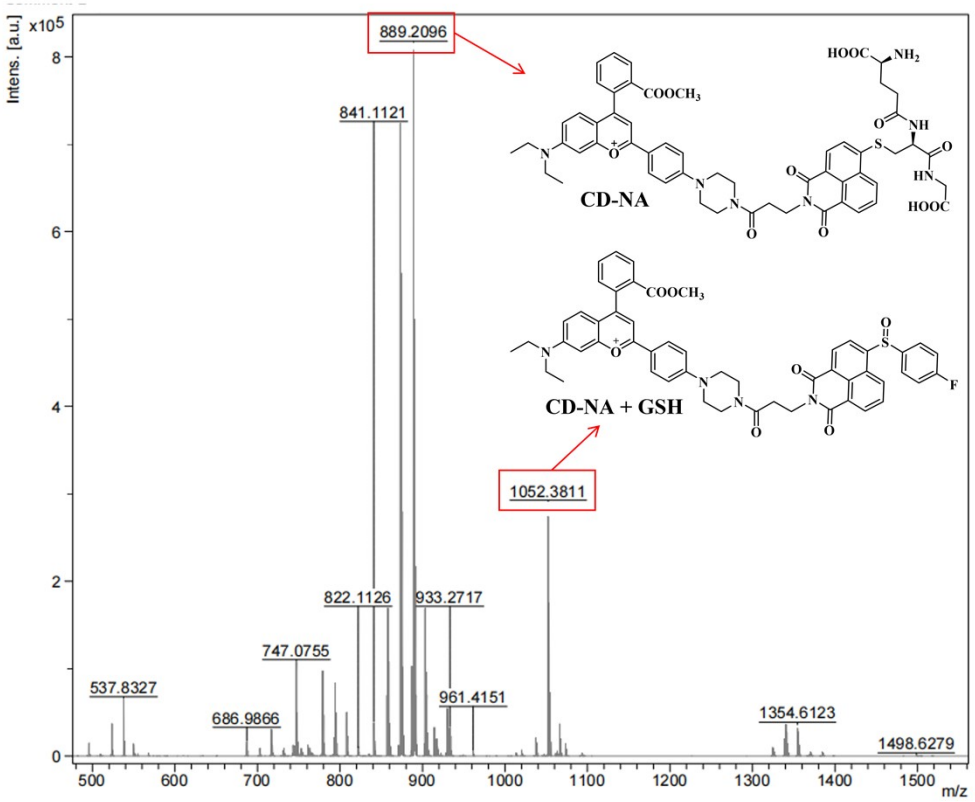

Figure S6. The mass spectrum of **CD-NA** in the presence of GSH.

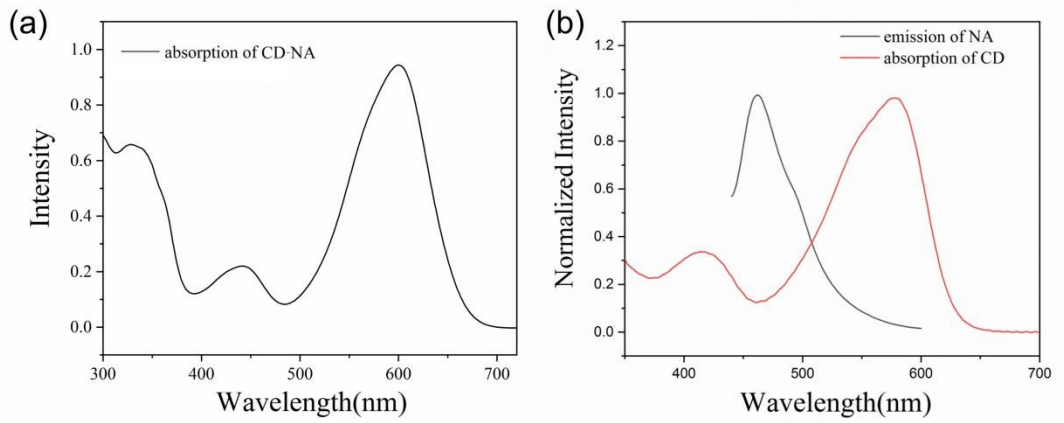

Figure S7. The absorption spectrum of **CD** (red) and the emission spectrum of **NA** (black).

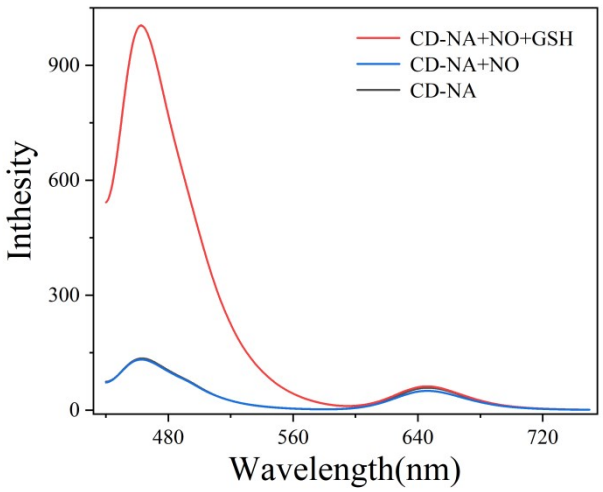

Figure S8. Fluorescence spectra of **CD-NA** (10 μM) with NO (0-200 μM) and GSH (0-5 mM) in PBS (0.01 M, 20% EtOH, pH 7.4)

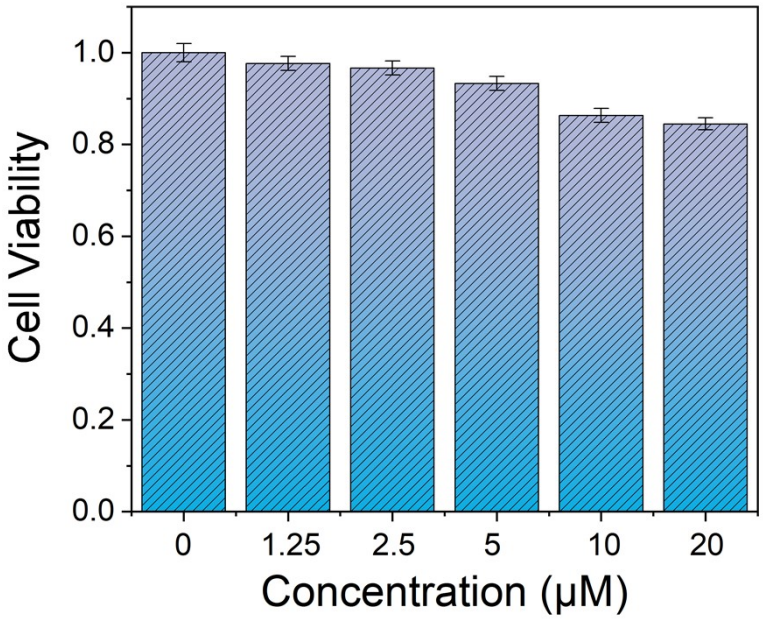

Figure S9. The cytotoxicity test of **CD-NA**.

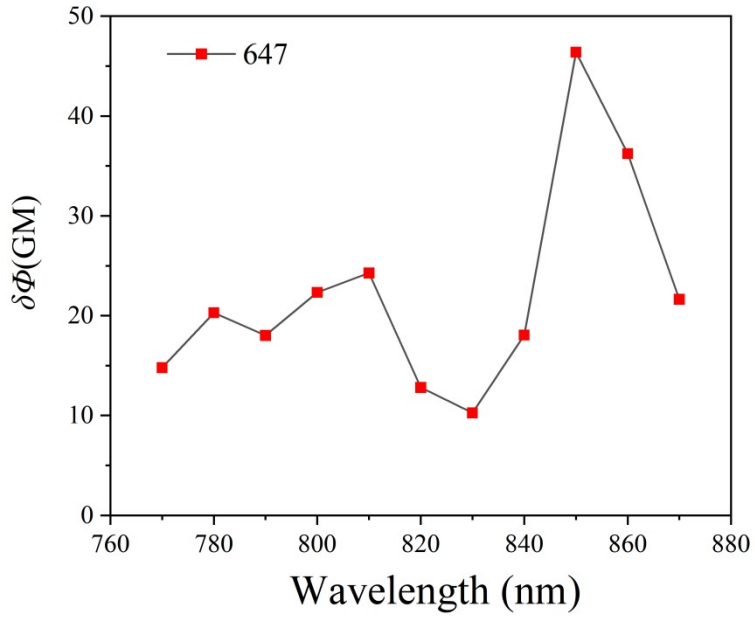

Figure S10. Two-photon excitation action cross-section of **CD-NA**.

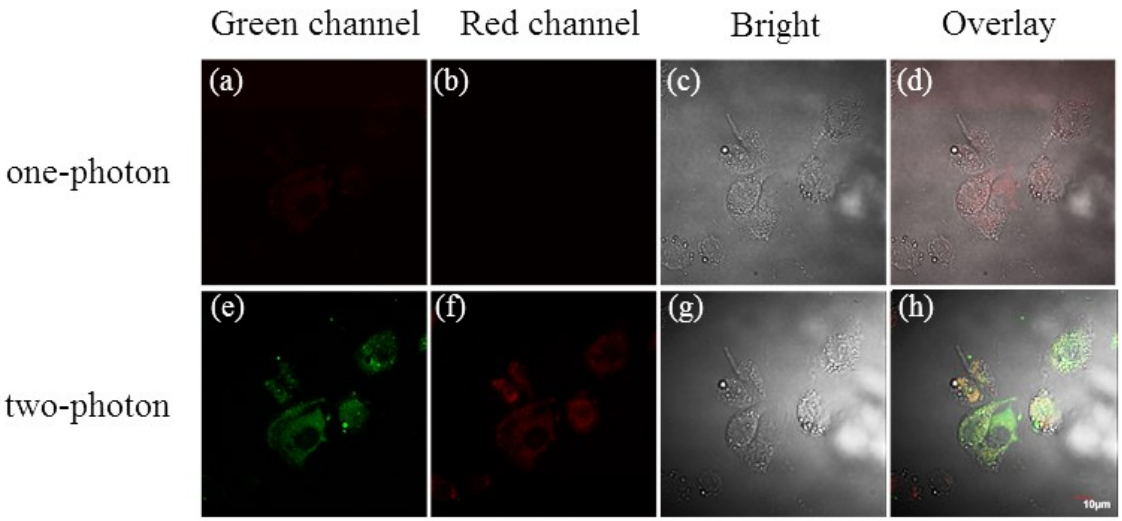

Figure S11. Images of HepG2 cells only incubated with **CD-NA** (5 μM) for 10 min by the one-photon and two-photon confocal fluorescence microscopy. Scale bar: 10 μm.

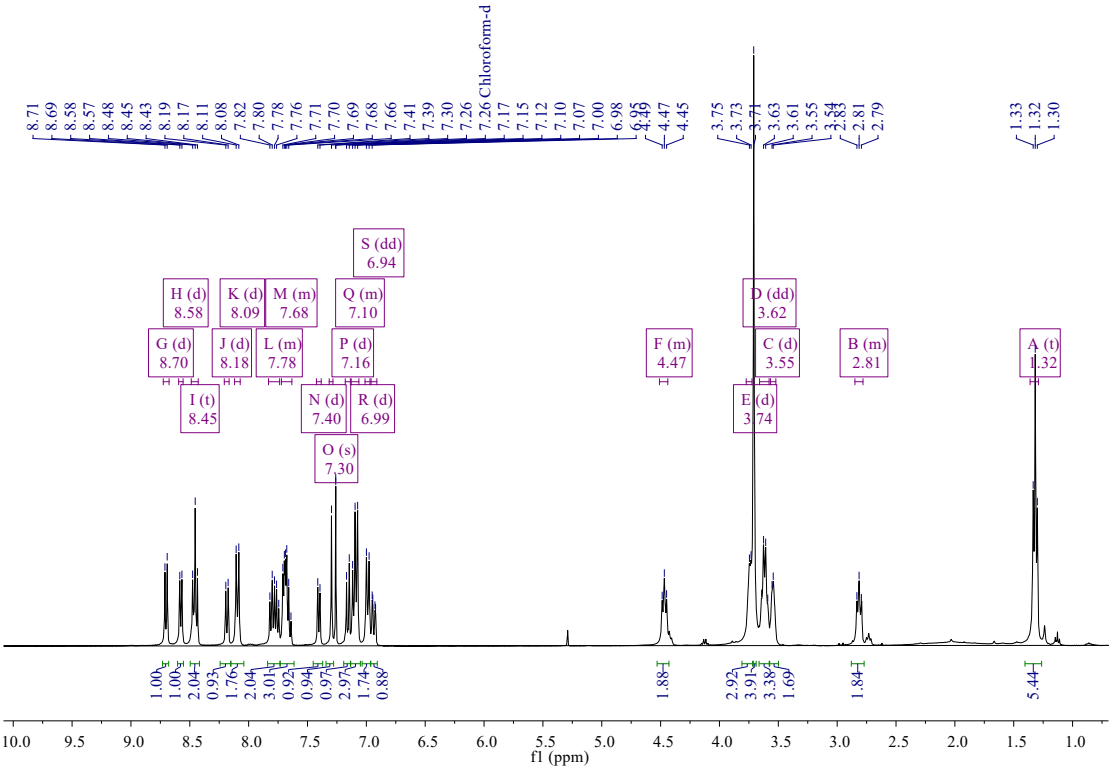

Figure S12. ^{1}H NMR spectrum of **CD-NA** (chloroform-d).

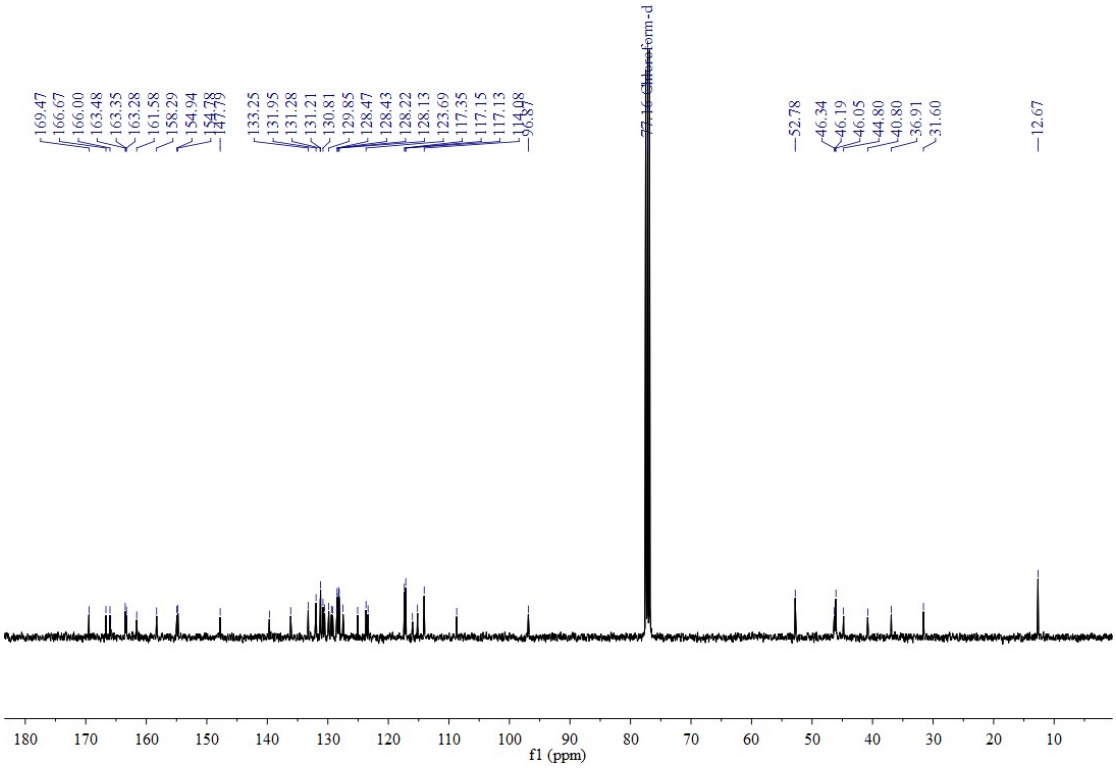

Figure S13. ^{13}C NMR spectrum of **CD-NA** (chloroform-d).

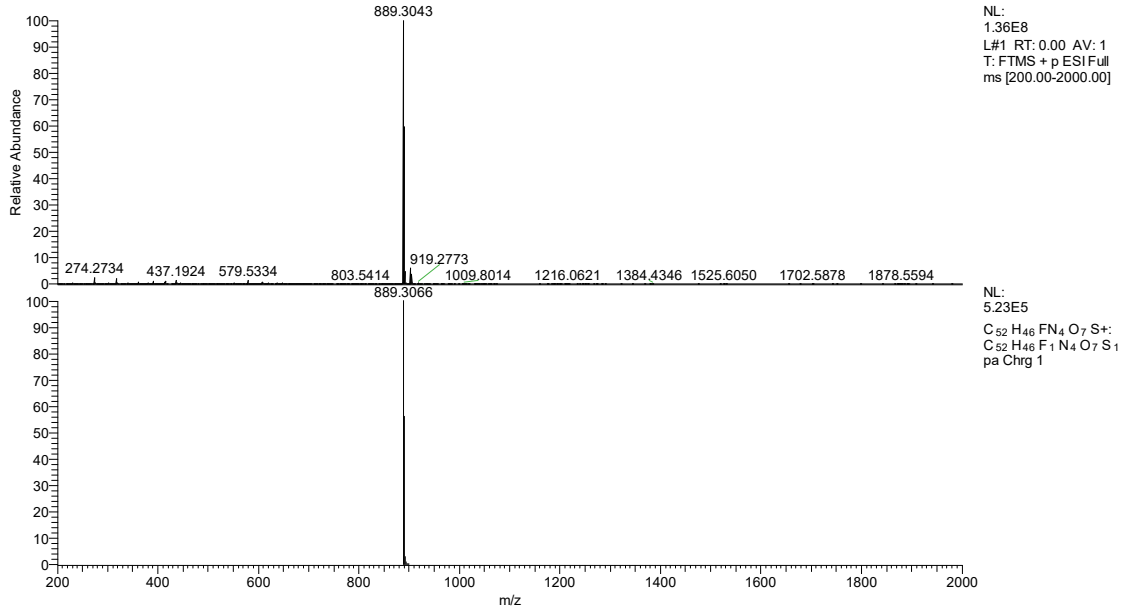

Figure S14. The HRMS spectrum of **CD-NA**.

References

[1] J. Zielonka, R. Podsiadły, M. Zielonka, M. Hardy, B. Kalyanaraman, On the use of peroxy-caged luciferin (PCL-1) probe for bioluminescent detection of inflammatory oxidants in vitro and in vivo – Identification of reaction intermediates and oxidant-specific minor products, Free Radical Biology and Medicine, 99(2016) 32-42.

[2] A. Sikora, J. Zielonka, M. Lopez, J. Joseph, B. Kalyanaraman, Direct oxidation of boronates by peroxynitrite: Mechanism and implications in fluorescence imaging of peroxynitrite, Free Radical Biology and Medicine, 47(2009) 1401-7.

[3] C. Jing, Y. Wang, X. Song, X. Li, Y. Feng, M. Kou, et al., A dual-fluorophore and dual-site multifunctional fluorescent sensor for real-time visualization of mitochondrial $ONOO^-$/GSH cross-talk in living cells, Sensors and Actuators B: Chemical, 365(2022) 131847.

[4] Y. Wang, Y. Liu, X. Song, Y. Feng, C. Jing, G. Zhang, et al., Dual-targetable fluorescent probe for mapping the fluctuation of peroxynitrite in drug-induced liver injury model, Spectrochimica Acta Part A: Molecular and Biomolecular Spectroscopy, 286(2023) 121892.

[5] Y. Wang, B. Li, X. Song, R. Shen, D. Wang, Y. Yang, et al., Mito-Specific Ratiometric Terbium(III)-Complex-Based Luminescent Probe for Accurate Detection of Endogenous Peroxynitrite by Time-Resolved Luminescence Assay, Analytical Chemistry, 91(2019) 12422-7.

[6] C. Jing, Y. Wang, X. Song, X. Li, M. Kou, G. Zhang, et al., Dual-Fluorophore and Dual-Site Multifunctional Fluorescence Sensor for Visualizing the Metabolic Process of GHS to SO_2 and the SO_2 Toxicological Mechanism by Two-Photon Imaging, Analytical Chemistry, 95(2023) 1376-84.